

On the dynamic distinguishability of nodal quasi-particles in overdoped cuprates

Kamran Behnia

LPEM (CNRS-Sorbonne University), ESPCI Paris, PSL University, 75005 Paris, France

(Dated: February 22, 2022)

$\text{La}_{1.67}\text{Sr}_{0.33}\text{CuO}_4$ is not a superconductor and its resistivity follows a purely T^2 temperature dependence at very low temperatures. $\text{La}_{1.71}\text{Sr}_{0.29}\text{CuO}_4$, on the other hand, has a superconducting ground state together with a T-Linear term in its resistivity. The concomitant emergence of these two features below a critical doping is mystifying. Here, I begin by noticing that the electron-electron collision rate in the Fermi liquid above the doping threshold is unusually large. Therefore, the scattering time of nodal quasi-particles is close to the threshold for dynamic indistinguishability, which is documented in liquid ^3He at its zero-temperature melting pressure. Failing this requirement of Fermi-Dirac statistics will exclude nodal electrons from the Fermi sea. Becoming classical, they will scatter other carriers within a phase space growing linearly with temperature.

I. Introduction

Elementary particles of a quantum fluid are indistinguishable. Leggett [1, 2] argued that it is thanks to this indistinguishability that such fluids are governed by quantum statistics [and not only quantum mechanics]. Trachenko and Zaconne [3, 4] recently highlighted the dynamical aspect of this indistinguishability and used it as a departing point to explore the boundary between the statistics-active and the statistics-inactive regimes of quantum fluids.

The normal state of cuprate superconductors is nowadays called a ‘strange metal’. The expression refers to the puzzling temperature dependence of their electrical resistivity (for recent reviews, see [5] and [6]). The focus of the present paper is a very specific point of the cuprate phase diagram. In hole-doped cuprates, the superconducting dome ends when doping level exceeds a threshold of $p \approx 0.3$. Hussey and collaborators carried out an extensive study of the evolution of resistivity in $\text{La}_{1-x}\text{Sr}_x\text{CuO}_4$ [7]. They found that the superconducting dome and strange metallicity emerge concomitantly when $x < 0.3$. $\text{La}_{1.67}\text{Sr}_{0.33}\text{CuO}_4$ is not superconducting and its resistivity follows T^2 [8], but $\text{La}_{1.71}\text{Sr}_{0.29}\text{CuO}_4$ is a superconductor and its resistivity does not correspond to what is expected for a Fermi liquid. Instead, it contains a T-Linear term [7] (Figure 1).

In this paper, I argue that the notion of dynamic distinguishability [4] illuminates the birth of a ‘strange metal’ at this locus of the phase diagram. The argument is based on scrutinizing the amplitude of T-square resistivity in the Fermi liquid $\text{La}_{1.67}\text{Sr}_{0.33}\text{CuO}_4$, by comparing it with other Fermi liquids, and by recalling the fate of fermion-fermion collisions when ^3He solidifies [9–12].

II. Heavily-doped LSCO stands out among Fermi liquids

$\text{La}_{1.67}\text{Sr}_{0.33}\text{CuO}_4$ is a Fermi liquid, but not a common one. This can be seen by comparing its T-square resistivity with other metallic oxides. In perovskite family, a variety of instabilities lead to metal-insulator transitions

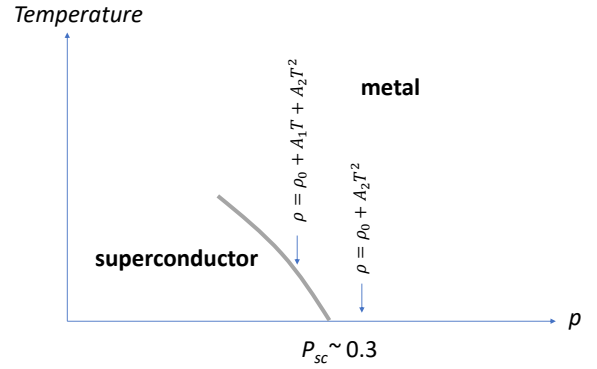


FIG. 1. **The puzzle:** Zoom on the cuprate phase diagram near the end of the superconducting dome. Hussey and his co-workers [7] found that below a threshold doping level, the system has a superconducting ground state and a resistivity which follows $\rho = \rho_0 + A_1 T + A_2 T^2$. Above this threshold, the system is not a superconductor and resistivity can be fit with a purely quadratic temperature-dependnet term: $\rho = \rho_0 + A_2 T^2$.

[13] and a metallic ground state is rare.

Let us pick up several exceptions. SrVO_3 is a correlated metal with vanadium in $3d^1$ configuration, which remains metallic when Sr is replaced by co-valent Ca [14]. SrTiO_3 is a band insulator and LaTiO_3 a Mott insulator, but $\text{Sr}_{1-x}\text{La}_x\text{TiO}_3$ alloys are metallic [15]. Specifically, $\text{Sr}_{0.05}\text{La}_{0.095}\text{TiO}_3$ is a dense metal with almost one electron per formula unit [15]. Sr_2RuO_4 is an unconventional superconductor with a Fermi liquid normal state above its critical temperature [16]. $\text{Sr}_3\text{Ru}_2\text{O}_7$ has a non-trivial electronic instability at 7.8 T, but is a correlated Fermi liquid at zero magnetic field [17, 18]. The feature they all share with $\text{La}_{1.67}\text{Sr}_{0.33}\text{CuO}_4$ is being a dense metallic perovskite. None of them, however, is a strange metal or become a high-temperature superconductor.

Fig. 2a shows the amplitude of the prefactor of T-square resistivity A as a function of the Sommerfeld co-

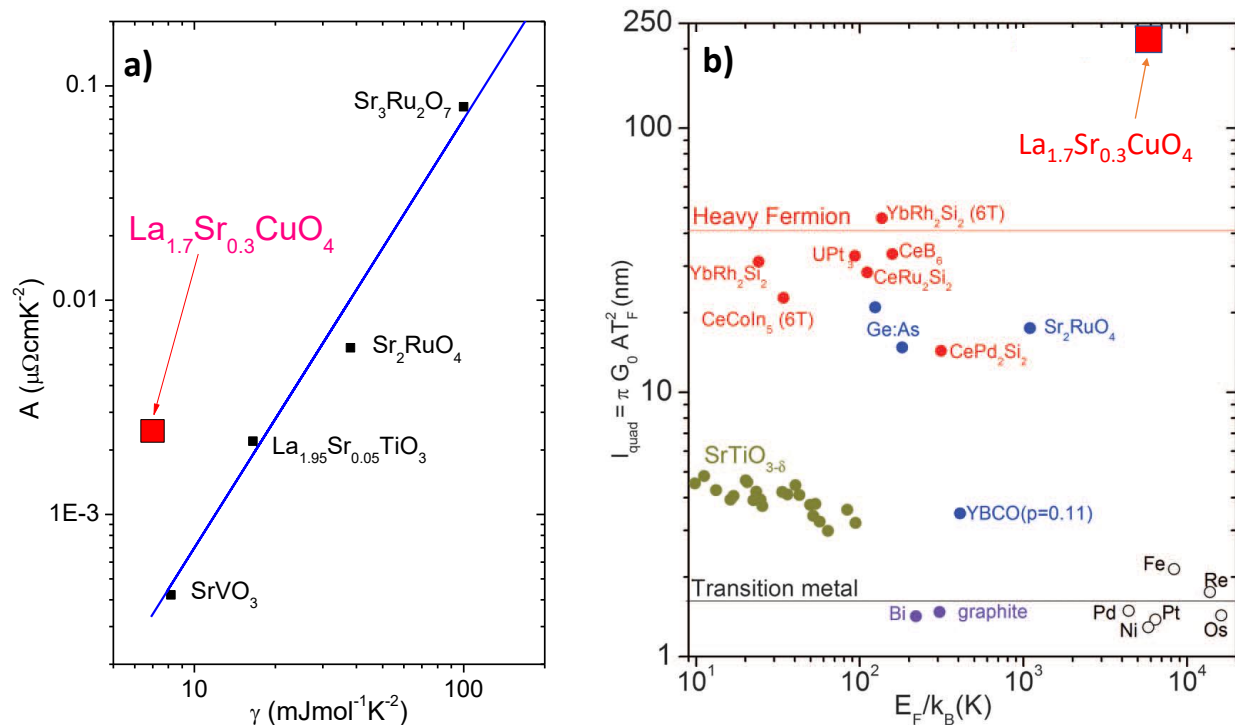


FIG. 2. **Standing out among Fermi liquids:** a) the magnitude of the prefactor of T-square resistivity, A , vs. the Sommerfeld coefficient, γ , of several metallic perovskites. SrVO_3 [14], Sr_2RuO_4 [19], $\text{Sr}_3\text{Ru}_2\text{O}_7$ (at zero magnetic field [17, 18]), and $\text{La}_{1.95}\text{Sr}_{0.05}\text{TiO}_3$ [15] all follow Kadowaki-Woods scaling. In contrast, the magnitude of A in $\text{La}_{1.67}\text{Sr}_{0.33}\text{CuO}_4$ [7, 8] is five times larger than what is expected given its γ . b) ℓ_{quad} , derived from the amplitude of A and fundamental constants (see text) in different Fermi liquids [20]. The large magnitude of ℓ_{quad} in $\text{La}_{1.67}\text{Sr}_{0.33}\text{CuO}_4$ stands out.

efficient (the electronic T-linear specific heat), γ in these metals. This Kadowaki-Woods (KW) plot [21] reveals an anomaly. In correlated metals, the prefactor of T-square resistivity scales with the square of γ over five orders of magnitude [22]. This scaling is operative when there is roughly one electron per formula unit [23]). As one can see in Fig. 2a, heavily-doped LSCO does not follow the trend observed in other metallic perovskites. Its T-square resistivity is more than five times larger than it should be, given the magnitude of its γ .

The unusually large amplitude of A betrays itself in yet another way and in a comparison of $\text{La}_{1.67}\text{Sr}_{0.33}\text{CuO}_4$ with *all* Fermi liquids. The Kadowaki-Woods scaling can be extended to dilute metals by plotting A as a function of the Fermi energy, E_F [20, 23, 24]. Due to Pauli exclusion principle, the phase space of scattering among fermions is proportional to $(\frac{k_B T}{E_F})^2$. Dimensional considerations imply:

$$A = \frac{\hbar}{e^2} \left(\frac{k_B}{E_F}\right)^2 \ell_{quad} \quad (1)$$

Here \hbar is the reduced Planck constant and e is the fundamental charge. ℓ_{quad} is a phenomenological material-dependent length scale. A survey of available data shows that for all known Fermi liquids ℓ_{quad} is between 1 to 50 nm [20, 24]. As one can see in Fig. 2b, in

$\text{La}_{1.67}\text{Sr}_{0.33}\text{CuO}_4$, $\ell_{quad} \approx 240$ nm. Decidedly, this Fermi liquid is not a banal one. The unusually large A of this metal, given its density of states and its degeneracy temperature is the first step for understanding its transformation to a strange metal with a superconducting ground state upon the removal of dopants.

To see the significance of this, let us consider the case of normal liquid ^3He .

III. Distinguishability on the verge of solidification in ^3He

Under their own vapor pressure, the two isotopes of helium do not solidify down to zero temperature. These quantum liquids [1, 2] become quantum solids upon the application of pressure. With an odd number of protons, neutrons and electrons, a ^3He atom is a composite fermion. The molar volume changes from 36.84 cm^3/mol at zero pressure to 25.5 cm^3/mol at $p=3.4$ MPa, when it solidifies. This is twice larger than what is classically expected (12 cm^3/mol) and is a consequence of the large zero-point motion of the atoms in the crystal [12].

The temperature dependence of thermal conductivity and viscosity in normal liquid ^3He at different pressures have been carefully measured by several authors. The quasi-particle scattering time extracted from these stud-

ies, broadly consistent with each other, were reviewed in detail by Dobbs [12]. The scattering time derived from thermal conductivity, τ_κ displays a T^{-2} behavior in the zero-temperature limit [9, 11], as expected for a Fermi liquid.

With increasing pressure, interaction between the atoms, consisting principally of a strong hard-core repulsion and a weak van der Waals attraction, intensifies. This leads to an amplification of the effective mass, quantified by measurements of specific heat [10] (Fig. 3a). Fig. 3b shows the evolution of $\tau_{kappa}T^2$ (in the zero-temperature limit) as a function of pressure reported by Wheatley [9] and by Greywall [11]. The trend is similar, but Greywall's values are 20-30 percent lower than Wheatley's. The highest pressure (3.44 MPa) corresponds to the onset of solidification. By this pressure, the time between two fermion-fermion collisions has decreased by a factor of almost 3.

Theoretical studies have examined the evolution of the effective mass and the Landau parameters found by experiment. Vollhardt, Wölfle and Anderson [25] employed a Hubbard model with a variable particle density to calculate the pressure dependence of the effective mass and the spin susceptibility. Pfitzner and Wölfle [26] found a reasonable account of transport coefficients at low pressure. These studies find that normal liquid ^3He is a strongly interacting and almost localized Fermi liquid [27], but localization does not occur up to the melting pressure [25].

What will be scrutinized here are the amplitudes of $\tau_\kappa T^2$ and the Fermi energy, E_F on the verge of solidification. According to Vollhardt and Wölfle [28], the quasi-particle lifetime on the Fermi surface is given by:

$$\tau_N^0 = \frac{64}{\pi^3} \frac{\hbar E_F}{(k_B T)^2} < W >_a^{-1} \quad (2)$$

$< W >_a$ is the angular average of the transition probabilities between spin singlet and spin triplet states [12, 28, 29]. Multiplying $\tau_{kappa}T^2$ by $\frac{k_B^2}{\hbar E_F}$ will yield a dimensionless number. This normalized quasi-particle lifetime is inversely proportional to the fermion-fermion collision strength.

Fig. 3c shows the evolution of the Fermi energy with pressure reconstructed from Greywall's data [11]. Combining this with $\tau_\kappa T^2$ leads to Fig. 3d, which shows the pressure dependence of $\frac{\tau_\kappa (k_B T)^2}{\hbar E_F}$. One can see that when solidification occurs, this number becomes as small as 0.015. Such a small normalized lifetime implies a huge collision rate between quasi-particles at the verge of solidification. Inserting this number in Eq. 2 leads to the conclusion that at the onset of solidification $< W >_a \approx 140$. Surprisingly, this remarkably large value has not been hitherto explicitly noticed, let alone commented.

Solid ^3He is far from a trivial solid. The zero-point motion is so large that each atom frequently encounters its first neighbours far from its lattice site. In other words, its anharmonicity is exceptionally large [30, 31].

However, this quantum solid is not subject to quantum statistics. Each atom is confined to the neighborhood of a designated site [32], even if it frequently exchanges this site with neighboring atoms by tunnelling. In contrast, in the liquid, the atoms are indistinguishable (See Fig. 4. Collisions in real space allow an atom to 'observe' its neighbours [33]. As these collisions multiply and confine the atom to a volume of the order of the unit cell, the indistinguishability becomes impossible.

Thus, the case of ^3He illustrates that when the time between two successive fermion-fermion collisions becomes unbearably short, the Fermi-Dirac statistics ceases to operate.

IV. Nodal quasiparticles: the unbearable shortness of being

What we just saw in the case of ^3He raises a question: Given the unusually large amplitude of the T-square resistivity in heavily doped LSCO, how short is the normalized quasi-particle lifetime?

Fig. 5a shows the Fermi surface of $\text{La}_{1.68}\text{Sr}_{0.32}\text{CuO}_4$ according to a tight binding model with nearest-neighbor hopping parameters chosen to fit the Fermi surface seen by Angle-Resolved Photoemission Spectroscopy (ARPES). [34–36]. The radius of this Fermi surface has a modest angular variation. In comparison, the angular variation of the Fermi velocity, v_F , is much larger (see Fig. 5b). This is a consequence of the proximity of Fermi surface and the Brillouin zone boundary along the anti-nodal direction. Because of the van Hove singularity, the evolution of the Fermi surface with doping differs along nodal and anti-nodal orientations. As a consequence v_F , the derivative of Fermi energy in momentum space, has a strong angular dependence.

In these conditions, nodal quasi-particles which have the fastest Fermi velocity, suffer the largest electron-electron collision rate. This can be seen by using the standard Drude expression for conductivity, $\rho^{-1} = \frac{ne^2\tau}{m^*}$ and finding :

$$\tau_\rho T^2 = A^{-1} \frac{\hbar}{e^2} \frac{2\pi c}{k_F v_F} \quad (3)$$

Here, $A = 2.5n\Omega cmK^{-2}$ is the experimentally measured T-square resistivity [7, 8], $c = 1.3nm$ is the c-axis lattice parameter. Since we are in presence of a two-dimensional Fermi surface, the carrier density is $n = \frac{k_F^2}{2\pi c}$. Since the anisotropy of k_F and v_F do not cancel out here, one expects a significant angle dependence of $\tau_\rho T^2$. As seen in Fig. 5c, this is indeed the case : $\tau_\rho T^2$ is more than twice smaller along the nodal orientation. Combining this with the Fermi energy $E_F = 5900K$, extracted from the magnitude of the T-linear electronic specific heat $\gamma = 6.9 \text{ mJ.mol}^{-1}.\text{K}^{-2}$ [8] leads to the dimensionless $(\tau_\rho k_B T)^2 / (\hbar E_F)$ and its angular dependence, shown in Fig. 5d. Along the nodal orientation, it becomes as

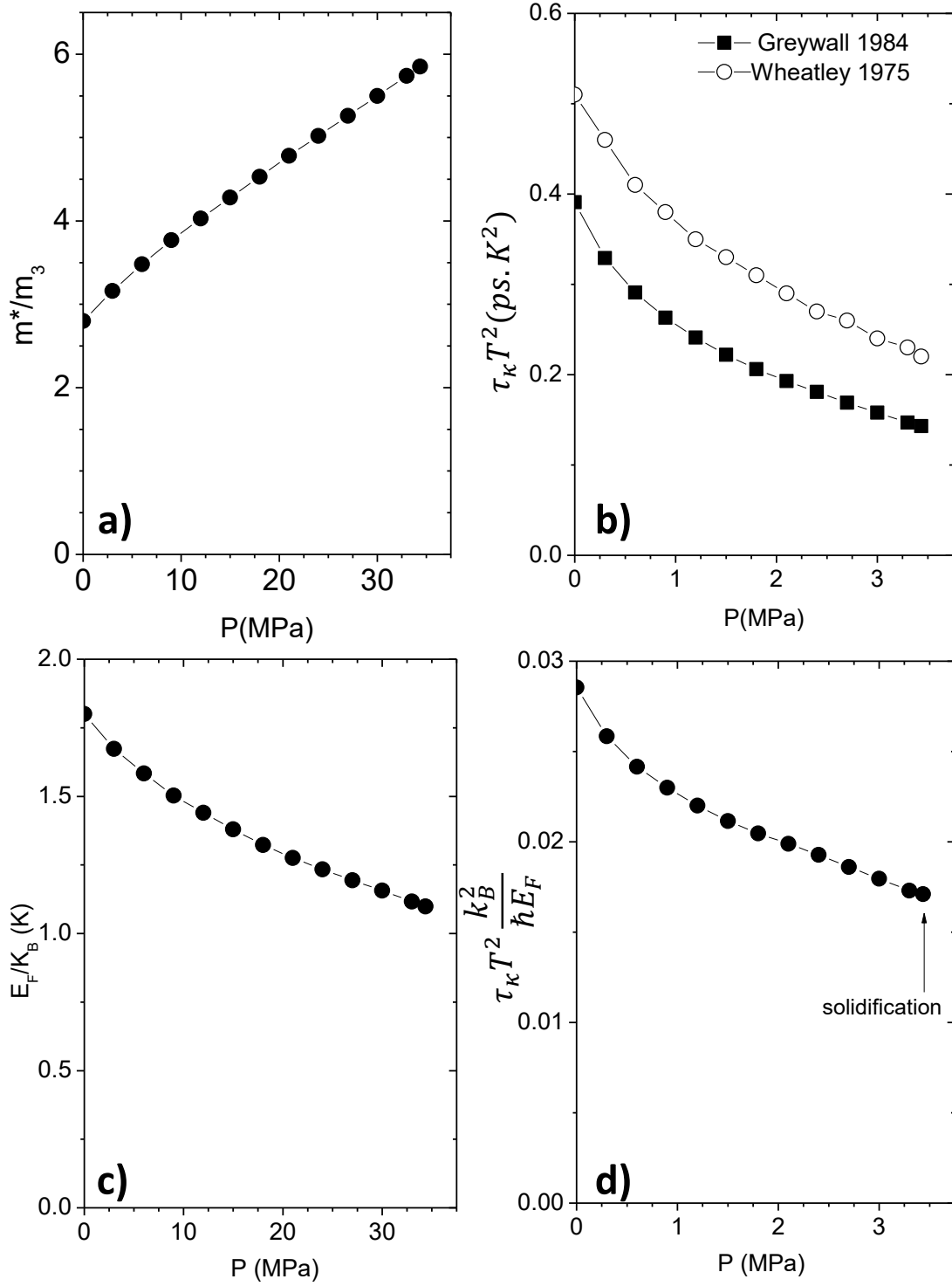


FIG. 3. **The case of normal liquid ${}^3\text{He}$** : a) The pressure dependence of the effective mass in ${}^3\text{He}$ quantified by measuring the T-linear specific heat [10]. b) The quasi-particle scattering time extracted from thermal conductivity multiplied by T^2 as a function of pressure, according to Wheatley [9] and Greywall [11]. c) The pressure dependence of the Fermi energy using the Fermi momentum and the Fermi velocity given by Greywall [11]. d) The pressure dependence of normalised quasiparticle lifetime using Greywall's data.

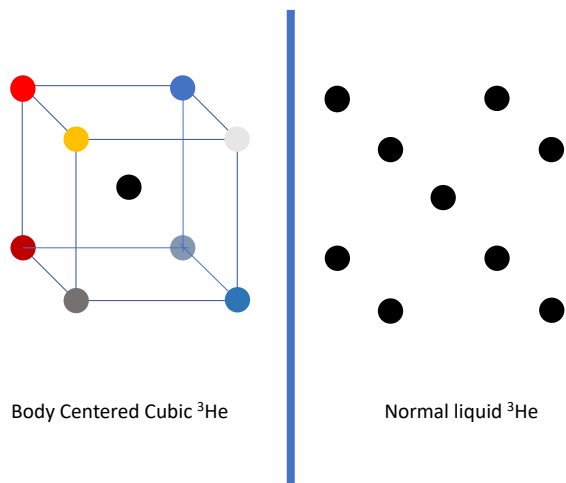


FIG. 4. **Discernability and indiscernability in ^3He** : Atoms in solid ^3He are distinguishable, because they are confined to specific sites in real space, even if, because of their large zero-point motion, they wander around, frequently exchanging their places with their neighbors. In contrast, atoms in liquid ^3He are indistinguishable. As a consequence, the number of configurations for collisions with first neighbours is larger by a factor of $Z!$ in the liquid, where Z is the coordination number.

small as 0.016, close to what was found above in ^3He on the verge of solidification.

The microscopic interaction is very different. In metals, point-like electrons repulse each other through screened Coulomb repulsion. In contrast, neutral ^3He atoms interact over a short range comparable to their hard-sphere radius and the interaction has both attractive and repulsive components. Nevertheless, the relative strength of fermion-fermion scattering rate (τ^{-1}) can be quantified in both cases by a dimensionless quantity defined as : $\zeta^{-1} = \tau \frac{(k_B T)^2}{\hbar E_F}$. As seen in table, $\zeta \gg 1$ in ^3He and in heavily-doped LSCO, but not in a weakly-interacting Fermi liquid, such as antimony [37]. Neglecting anisotropy, one can show that the dimensionless ζ is proportional to the phenomenological length scale ℓ_{quad} defined by Eq. 1 :

$$\zeta = \frac{\ell_{quad}}{\ell_{dd}} \quad (4)$$

In three dimensions, ℓ_d is proportional to the Fermi wavelength $\ell_{3d} = 3\pi\lambda_F$, and in two dimensions, to the c-axis lattice parameter: $\ell_{2d} = 4\pi c$. In heavily overdoped LSCO, ℓ_{quad} and ζ are unusually large. If there is an upper boundary to ζ , nodal quasi-particles in cuprates will encounter it first.

Let us assume that at the threshold doping, an exceedingly large rate of fermion-fermion collision rate makes the nodal quasi-particles distinguishable, freezing them out of the Fermi sea.

V. Consequences of nodal freeze-out

If the nodal quasi-particles become excluded from the Fermi sea below the threshold doping, two categories of electrons [38] will co-exist: Those for which quantum statistics is non-operative and the others remaining in the Fermi sea. The consequences of this dichotomy in real space are unknown. Yet, this hypothesis will provide new possible solutions to a number of longstanding puzzles. They are listed below:

- **Planckian dissipation:** Bruin and co-workers noticed that in many metals with a T-linear resistivity, the amplitude of scattering time is of the order of $\tau_P = \frac{\hbar}{k_B T}$ [39]. Legros and co-workers [40] have reported that this indeed the case of overdoped cuprates. This so-called ‘Planckian dissipation’ is encountered in variety of contexts in both conventional and unconventional metals [41]. A scattering time of the order of $\sim \frac{\hbar}{k_B T}$ is expected when degenerate electrons are scattered off classical objects. The latter may be phonons above in the vicinity or above their Debye temperature or electrons in the vicinity or above their Fermi temperature. The latter option, was employed to explain the strange metallicity of $\text{Sr}_3\text{Ru}_2\text{O}_7$ [42]. Mousatov and co-workers showed that in this system, T-linear resistivity and its Planckian prefactor [39] can be explained by invoking the scattering of the degenerate electrons of a large pocket by the classical electrons of a small pocket. Such a scenario may be relevant to other correlated metals, but not to cuprates, which have a single Fermi pocket. On the other hand, if nodal quasi-particles become classical because of their distinguishability, then the Planckian dissipation will find a straightforward explanation.
- **Isotropic T^{-1} scattering rate:** Grissonnanche and co-workers [43] have recently reported that the T-linear scattering is independent of direction. This isotropy would not be surprising if the underlying mechanism is the scattering of quantum-mechanically degenerate electrons by classical nodal electrons, which are distributed along two orthogonal orientations and $\cos^2(\phi) + \cos^2(\phi + \pi/2)$ does not vary with θ .
- **Saturation of the amplitude of the T-square prefactor:** Cooper and co-workers [7] find that the amplitude of A_2 , the prefactor of T-square resistivity does not evolve with doping in the strange metal. This behavior is in striking contrast with what is seen in quantum-critical metals [44, 45]. On the other hand, it would be expected if the magnitude of electron-electron scattering has attained a ceiling.
- **The evolution of carrier density with doping:** Experiments [46, 47] find that the Hall carrier density gradually decreases from $1 + p$ at high

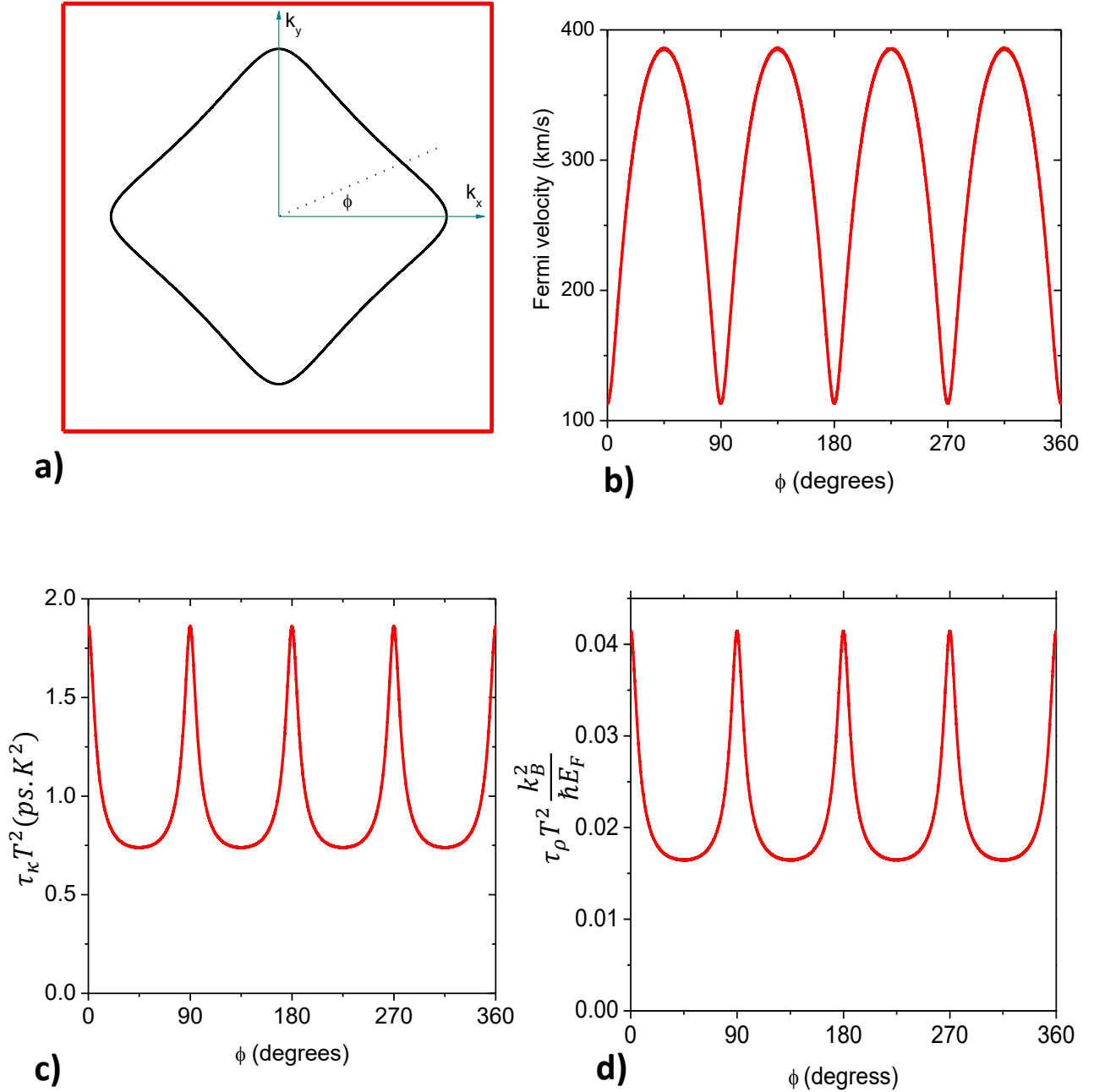


FIG. 5. **Angular variation of collision time in heavily overdoped LSCO:** a) Fermi surface and the Brillouin zone of $\text{La}_{1.68}\text{Sr}_{0.32}\text{CuO}_4$; b) Angular variation of the Fermi velocity; c) Angular variation of the scattering time derived from resistivity times T^2 ; d) Angular dependence of $\tau_\rho T^2$ normalized by $\frac{k_B^2}{\hbar E_F}$. Compare the absolute value of the minima for nodal orientations with what was seen in the case of ^3He .

System	Carrier density (m^{-3})	m^*/m_0	E_F (K)	τT^2 (s.K ²)	ζ
^3He (p=0)	1.63×10^{28}	2.8	1.8	3.9×10^{-13}	21
^3He (p=3.4MPa)	2.36×10^{28}	2.8	1.1	1.4×10^{-13}	60
$\text{La}_{1.67}\text{Sr}_{0.33}\text{CuO}_4$	7.4×10^{27}	5	5900	$0.7\text{-}1.8 \times 10^{-9}$	24-61
Sb	1.1×10^{26}	0.07-1	1100	$1.5\text{-}3 \times 10^{-8}$	0.5-1

TABLE I. ^3He and heavily-doped LSCO compared to a weakly correlated Fermi liquid semi-metallic antimony [37]. The normalized amplitude of fermion-fermion scattering in the latter is close to unity.

doping to p at low doping. On the other hand, the superfluid density does not show any sharp feature as a function of doping and shows a dome-like structure similar to the critical temperature [48], as found in a conventional superconductor [49]. If with decreasing carrier density, a larger fraction of electrons is peeled off the Fermi surface, but the superfluid density keeps to be zero along the nodal direction, the discrepancy becomes less surprising.

- **Nodal excitons:** Being extracted off the Fermi sea, nodal electrons and nodal holes can pair up and form excitons. Such bosons are plausible candidates for playing the role of pair-forming bosons. Such a mechanism for the formation of pairs has been already proposed in other contexts [50], but not in cuprates. The superconducting order parameter would naturally vanish along the nodal orientations, in conformity with the d-wave symmetry of cuprates [51].

VI. Concluding remarks

The present paper reports on two observations and on a speculation.

The observations are about the amplitude of fermion-fermion scattering in two different strongly correlated fermionic systems: ^3He atoms near the melting pressure and nodal quasi-particles in cuprates on the verge of superconductivity. The dimensionless amplitudes is strikingly similar and fermion-fermion collision rate in liquid ^3He is near the threshold of distinguishability.

The speculation is that the collision rate in the cuprate is also near a threshold which would render a subset of fermions distinguishable. If this happens to be the case, the exclusion of this subset of fermions from the Fermi sea will provide plausible explanations for the sudden emergence of T-linear resistivity and a robust superconducting ground state.

The present approach may also prove relevant to deciphering the passage from T-square to T-linear resistivity in graphene [52].

-
- [1] A. J. Leggett, *Quantum Liquids: Bose condensation and Cooper pairing in condensed-matter systems* (Oxford University Press, 2006).
- [2] A. J. Leggett, *Science* **319**, 1203 (2008), <https://www.science.org/doi/pdf/10.1126/science.1152822>.
- [3] K. Trachenko, arXiv e-prints, arXiv:2104.07422 (2021), arXiv:2104.07422 [quant-ph].
- [4] A. Zaccane and K. Trachenko, Dynamical indistinguishability and statistics in quantum fluids (2021), arXiv:2107.09995 [quant-ph].
- [5] N. E. Hussey, J. Buhot, and S. Licciardello, *Reports on Progress in Physics* **81**, 052501 (2018).
- [6] C. Proust and L. Taillefer, *Ann. Rev. Condens. Matt. Phys.* **10**, 409 (2019).
- [7] R. A. Cooper, Y. Wang, B. Vignolle, O. J. Lipscombe, S. M. Hayden, Y. Tanabe, T. Adachi, Y. Koike, M. Nohara, H. Takagi, C. Proust, and N. E. Hussey, *Science* **323**, 603 (2009).
- [8] S. Nakamae, K. Behnia, N. Mangkorntong, M. Nohara, H. Takagi, S. J. C. Yates, and N. E. Hussey, *Phys. Rev. B* **68**, 100502 (2003).
- [9] J. C. Wheatley, *Rev. Mod. Phys.* **47**, 415 (1975).
- [10] D. S. Greywall, *Phys. Rev. B* **27**, 2747 (1983).
- [11] D. S. Greywall, *Phys. Rev. B* **29**, 4933 (1984).
- [12] E. R. Dobbs, *Helium Three* (Oxford University Press, 2000).
- [13] M. Imada, A. Fujimori, and Y. Tokura, *Rev. Mod. Phys.* **70**, 1039 (1998).
- [14] I. H. Inoue, O. Goto, H. Makino, N. E. Hussey, and M. Ishikawa, *Phys. Rev. B* **58**, 4372 (1998).
- [15] Y. Tokura, Y. Taguchi, Y. Okada, Y. Fujishima, T. Arima, K. Kumagai, and Y. Iye, *Phys. Rev. Lett.* **70**, 2126 (1993).
- [16] A. P. Mackenzie and Y. Maeno, *Rev. Mod. Phys.* **75**, 657 (2003).
- [17] S. A. Grigera, R. S. Perry, A. J. Schofield, M. Chiao, S. R. Julian, G. G. Lonzarich, S. I. Ikeda, Y. Maeno, A. J. Millis, and A. P. Mackenzie, *Science* **294**, 329 (2001), <https://www.science.org/doi/pdf/10.1126/science.1063539>.
- [18] A. W. Rost, S. A. Grigera, J. A. N. Bruin, R. S. Perry, D. Tian, S. Raghu, S. A. Kivelson, and A. P. Mackenzie, *Proceedings of the National Academy of Sciences* **108**, 16549 (2011), <https://www.pnas.org/content/108/40/16549.full.pdf>.
- [19] Y. Maeno, K. Yoshida, H. Hashimoto, S. Nishizaki, S.-i. Ikeda, M. Nohara, T. Fujita, A. Mackenzie, N. Hussey, J. Bednorz, and F. Lichtenberg, *Journal of the Physical Society of Japan* **66**, 1405 (1997), <https://doi.org/10.1143/JPSJ.66.1405>.
- [20] X. Lin, B. Fauqué, and K. Behnia, *Science* **349**, 945 (2015).
- [21] K. Kadowaki and S. Woods, *Solid State Communications* **58**, 507 (1986).
- [22] N. Tsujii, K. Yoshimura, and K. Kosuge, *Journal of Physics: Condensed Matter* **15**, 1993 (2003).
- [23] K. Behnia, On the origin and the amplitude of T-square resistivity in Fermi liquids (2021), arXiv:arXiv:2112.11092 [cond-mat.str-el].
- [24] J. Wang, J. Wu, T. Wang, Z. Xu, J. Wu, W. Hu, Z. Ren, S. Liu, K. Behnia, and X. Lin, *Nature Communications* **11**, 3846 (2020).
- [25] D. Vollhardt, P. Wölfle, and P. W. Anderson, *Phys. Rev. B* **35**, 6703 (1987).
- [26] M. Pfizner and P. Wölfle, *Phys. Rev. B* **35**, 4699 (1987).
- [27] D. Vollhardt, *Rev. Mod. Phys.* **56**, 99 (1984).
- [28] D. Vollhardt and P. Wölfle, *The superfluid phases of helium 3* (CRC Press, 1990).
- [29] P. Wolfe, *Reports on Progress in Physics* **42**, 269 (1979).
- [30] R. A. Guyer and L. I. Zane, *Phys. Rev.* **188**, 445 (1969).
- [31] R. A. Guyer, R. C. Richardson, and L. I. Zane, *Rev. Mod. Phys.* **43**, 532 (1971).
- [32] D. J. Thouless, *Proceedings of the Physical Society* **86**,

- 893 (1965).
- [33] A. Smerzi, *Phys. Rev. Lett.* **109**, 150410 (2012).
- [34] T. Yoshida, X. J. Zhou, K. Tanaka, W. L. Yang, Z. Husain, Z.-X. Shen, A. Fujimori, S. Sahrakorpi, M. Lindroos, R. S. Markiewicz, A. Bansil, S. Komiyama, Y. Ando, H. Eisaki, T. Kakeshita, and S. Uchida, *Phys. Rev. B* **74**, 224510 (2006).
- [35] M. Horio, K. Hauser, Y. Sassa, Z. Mingazheva, D. Sutter, K. Kramer, A. Cook, E. Nocerino, O. K. Forsslund, O. Tjernberg, M. Kobayashi, A. Chikina, N. B. M. Schröter, J. A. Krieger, T. Schmitt, V. N. Strocov, S. Pyon, T. Takayama, H. Takagi, O. J. Lipscombe, S. M. Hayden, M. Ishikado, H. Eisaki, T. Neupert, M. Månsson, C. E. Matt, and J. Chang, *Phys. Rev. Lett.* **121**, 077004 (2018).
- [36] H. Jin, A. Narduzzo, M. Nohara, H. Takagi, N. E. Hussey, and K. Behnia, *Journal of the Physical Society of Japan* **90**, 053702 (2021), <https://doi.org/10.7566/JPSJ.90.053702>.
- [37] A. Jaoui, B. Fauqué, and K. Behnia, *Nature Communications* **12**, 195 (2021).
- [38] For an alternative scenario referring to two distinct (coherent and incoherent) charge sectors see [53]. Note the very different nature of electron dichotomy in the two scenarios.
- [39] J. A. N. Bruin, H. Sakai, R. S. Perry, and A. P. Mackenzie, *Science* **339**, 804 (2013), <https://www.science.org/doi/pdf/10.1126/science.1227612>.
- [40] A. Legros, S. Benhabib, W. Tabis, F. Laliberté, M. Dion, M. Lizaire, B. Vignolle, D. Vignolles, H. Raffy, Z. Z. Li, P. Auban-Senzier, N. Doiron-Leyraud, P. Fournier, D. Colson, L. Taillefer, and C. Proust, *Nature Physics* **15**, 142 (2019).
- [41] S. A. Hartnoll and A. P. Mackenzie, *arXiv e-prints*, [arXiv:2107.07802](https://arxiv.org/abs/2107.07802) (2021), [arXiv:2107.07802](https://arxiv.org/abs/2107.07802) [cond-mat.str-el].
- [42] C. H. Mousatov, E. Berg, and S. A. Hartnoll, *Proceedings of the National Academy of Sciences* **117**, 2852 (2020), <https://www.pnas.org/content/117/6/2852.full.pdf>.
- [43] G. Grissonnanche, Y. Fang, A. Legros, S. Verret, F. Laliberté, C. Collignon, J. Zhou, D. Graf, P. A. Goddard, L. Taillefer, and B. J. Ramshaw, *Nature* **595**, 667 (2021).
- [44] J. Custers, P. Gegenwart, H. Wilhelm, K. Neumaier, Y. Tokiwa, O. Trovarelli, C. Geibel, F. Steglich, C. Pépin, and P. Coleman, *Nature* **424**, 524 (2003).
- [45] J. Paglione, M. A. Tanatar, D. G. Hawthorn, E. Boaknin, R. W. Hill, F. Ronning, M. Sutherland, L. Taillefer, C. Petrovic, and P. C. Canfield, *Phys. Rev. Lett.* **91**, 246405 (2003).
- [46] S. Badoux, W. Tabis, F. Laliberté, G. Grissonnanche, B. Vignolle, D. Vignolles, J. Béard, D. A. Bonn, W. N. Hardy, R. Liang, N. Doiron-Leyraud, L. Taillefer, and C. Proust, *Nature* **531**, 210 (2016).
- [47] C. Putzke, S. Benhabib, W. Tabis, J. Ayres, Z. Wang, L. Malone, S. Licciardello, J. Lu, T. Kondo, T. Takeuchi, N. E. Hussey, J. R. Cooper, and A. Carrington, *Nature Physics* **17**, 826 (2021).
- [48] I. Božović, X. He, J. Wu, and A. T. Bollinger, *Nature* **536**, 309 (2016).
- [49] C. Collignon, B. Fauqué, A. Cavanna, U. Gennser, D. Maily, and K. Behnia, *Phys. Rev. B* **96**, 224506 (2017).
- [50] A. Kavokin and P. Lagoudakis, *Nature Materials* **15**, 599 (2016).
- [51] C. C. Tsuei and J. R. Kirtley, *Rev. Mod. Phys.* **72**, 969 (2000).
- [52] A. Jaoui, I. Das, G. Di Battista, J. Díez-Mérida, X. Lu, K. Watanabe, T. Taniguchi, H. Ishizuka, L. Levitov, and D. K. Efetov, *arXiv e-prints* **2105.08408** (2021).
- [53] M. Culo, C. Duffy, J. Ayres, M. Berben, Y.-T. Hsu, R. D. H. Hinlopen, B. Bernath, and N. E. Hussey, *SciPost Phys.* **11**, 12 (2021).